The Plant Cell, Vol. 8, 1193–1207, July 1996

A Nuclear Mutant of Arabidopsis with Impaired Stability on Distinct Transcripts of the Plastid *psbB*, *psbD/C*, *ndhH*, and *ndhC* Operons

Jörg Meurer, Anja Berger, and Peter Westhoff[1]

Institut für Entwicklungs- und Molekularbiologie der Pflanzen, Heinrich-Heine-Universität, Universitätsstrasse 1, D-40225 Düsseldorf, Germany

The high-chlorophyll fluorescence photosynthesis mutant *hcf109* of Arabidopsis was characterized in detail to gain insights into the regulatory mechanism of RNA processing in higher plants. By using electron transport, chlorophyll fluorescence, and immunoblot studies, we assigned the mutational lesion to photosystems I and II and the plastid NAD(P)H dehydrogenase complex. The functional pleiotropy was reflected in RNA deficiencies. Although all nuclear-encoded photosynthetic RNAs analyzed revealed no difference in size or steady state level between mutant and wild type, the RNA patterns of the plastome-encoded *psbB-psbT-psbH-petB-petD*, *psbD-psbC-ycf9*, *ndhC-ndhK-ndhJ*, and *ndhH-ndhA-ndhI-ndhG-ndhE-psaC-ndhD* transcription units were severely disturbed. These operons encode subunits of photosystems I (*psa*) and II (*psb*), the cytochrome b_6f complex (*pet*), the plastid NAD(P)H dehydrogenase (*ndh*), and the unidentified open reading frame *ycf9*. With the exception of the *ndhC* operon, the RNA deficiencies observed were specific and restricted to particular segments of the *psbB*, *psbD/C*, and *ndhH* operons, that is, the *psbB-psbT*, *ycf9*, and *psaC* regions. Run-on transcription studies with isolated chloroplasts showed that the failure of these transcripts to accumulate was due to RNA stability and not transcription. Other polycistronic transcription units analyzed were not affected by the mutation. This result indicates that the *trans*-regulatory factor encoded by the *hcf109* gene is not a general RNA stability factor but that it specifically controls the stability of only these distinct transcripts. Because the *hcf109* locus was mapped at a distance <0.1 centimorgans from the phytochrome C gene, its molecular characterization by positional cloning is possible.

INTRODUCTION

Polycistronic transcription units are typical for plastid gene organization in land plants (Herrmann et al., 1992; Ohyama, 1992; Palmer, 1992; Sugiura, 1992). The genetic composition of these units is often heterogenous and reflects their postendosymbiotic assembly from disparate cyanobacterial progenitor operons or genes (Douglas, 1994). The evolutionary reorganizations in operon structure may also explain, at least partially, the highly complex transcript patterns that are usually observed with plastid polycistronic transcription units (Berends et al., 1987; Hudson et al., 1987; Matsubayashi et al., 1987; Barkan, 1988; Westhoff and Herrmann, 1988). Most of the detectable transcript complexity is probably due to RNA processing; that is, endonucleases and exonucleases as well as splicing activities act on the primary polycistronic transcripts to generate oligocistronic RNAs. However, several examples demonstrate that multiple transcription initiation contributes to transcript complexity and may even be its primary cause (Woodbury et al., 1989; Yao et al., 1989; Haley and Bogorad, 1990; Christopher et al., 1992; Kapoor et al., 1994).

The functional significance of RNA processing for the control of plastid gene expression is poorly understood. A priori processing of polycistronic transcripts into oligocistronic RNAs is not a prerequisite for translation initiation to occur. For instance, the polycistronic transcripts of the *psbB* operon, which encodes the three photosystem II genes *psbB*, *psbT*, and *psbH*, and the two cytochrome b_6f complex genes *petB* and *petD* (Barkan, 1988; Westhoff and Herrmann, 1988; Monod et al., 1994) are assembled into polysomes, which suggests that they function as mRNAs (Barkan, 1988). However, oligocistronic and monocistronic RNAs may be far better templates for translation initiation than their polycistronic precursors. This is illustrated by the high-chlorophyll fluorescence (*hcf*) mutant *crp1* (chloroplast RNA processing) of maize, which is affected in generating the monocistronic *petB* and *petD* RNAs (Barkan et al., 1994). The translational efficiency of plastid RNAs also can be influenced by processing the 5′ untranslated leader regions (Reinbothe et al., 1993).

Processing polycistronic transcripts into oligocistronic RNAs is necessary if individual segments of primary polycistronic transcripts are to accumulate at different levels. This post-

[1] To whom correspondence should be addressed.

transcriptional mode of gene regulation is well documented in prokaryotes and is based on segmental variations in RNA stability (von Gabain et al., 1983; Newbury et al., 1987; Båga et al., 1988; Chen et al., 1988; Eddy et al., 1991). A differential accumulation of the component RNAs of the *psbB* transcription units has been reported recently for mesophyll and bundle-sheath chloroplasts of monocotyledonous C_4 plants (Westhoff et al., 1991; Kubicki et al., 1994). However, whether differential RNA stability is its sole cause has not been determined.

The biochemical basis of RNA processing and stability in plastids is beginning to be elucidated. Cleaving polycistronic precursor transcripts into mature RNAs requires endonucleases that recognize specific sequences and/or structures. Endonucleolytic cleavage points have been mapped in the intercistronic regions of polycistronic transcripts (Westhoff and Herrmann, 1988; Barkan et al., 1994), but the molecular nature of the endonucleolytic activities involved is still to be discovered. This contrasts with a fairly large body of available information on RNA 3′ end maturation (reviewed in Gruissem and Schuster, 1993; Mayfield et al., 1995). Exonucleolytic and endonucleolytic activities, which act upon immature 3′ ends and the corresponding *cis*-acting sequences, have been identified (Stern and Gruissem, 1987; Chen and Stern, 1991; Nickelsen and Link, 1993). It has been demonstrated by in vitro and in vivo approaches that the stem–loop structures located at RNA 3′ ends and their neighboring regions function as processing elements. These portions of the 3′ untranslated regions are also necessary for stabilizing upstream RNA sequences (Stern and Gruissem, 1987; Stern et al., 1991; Blowers et al., 1993). However, in vivo experiments with Chlamydomonas indicate that the 5′ untranslated regions of mRNAs have a much more profound effect on RNA stability than do their 3′ counterparts (Sakamoto et al., 1993; Salvador et al., 1993). The 3′ and/or the 5′ untranslated regions of plastid RNAs have been shown to be targets of RNA binding proteins, which are involved in processing and/or stabilization of particular RNAs (Li and Sugiura, 1991; Schuster and Gruissem, 1991; Nickelsen et al., 1994).

We are interested in understanding the functional significance of RNA processing and stability for the regulation of plastid gene expression in higher plants. Our research is based on a genetic approach, with Arabidopsis as the experimental organism. By using the *hcf* phenotype as a selection criterion (Miles, 1980, 1982), we started a systematic search for mutants defective in photosynthetic light reactions and electron transport. To date, 34 recessive nuclear Arabidopsis mutants generated by mutagenesis with ethyl methanesulfonate have been isolated and characterized by chlorophyll fluorescence induction, P700 absorption kinetics, and immunoblotting (Meurer et al., 1996). Here, the detailed characterization of mutant *hcf109* is reported. By using photosynthetic electron transport measurements, 77K fluorescence spectra, immunoblotting, and in vivo labeling experiments, we show that this mutant is affected in photosystems I and II and the plastid NAD(P)H dehydrogenase complex. RNA gel blot and transcription run-on analyses demonstrated that this mutant is unable to accumulate distinct transcripts of four polycistronic transcription units, the *psbB*, *psbD/C*, *ndhH*, and *ndhC* operons, whereas RNA accumulation in other plastid operons is not affected. It follows that the *hcf109* gene does not encode a general RNA stability factor but rather a *trans*-regulatory component that specifically and concomitantly controls the stability of distinct transcripts.

RESULTS

Photosynthetic Electron Transport and Spectroscopic Measurements Show Impaired Photosystem I and II Complexes in *hcf109*

The mutant *hcf109* was isolated as a recessive high-chlorophyll fluorescence mutant from a collection of 7700 individual M_2 families that were generated by ethyl methanesulfonate mutagenesis of Arabidopsis seeds (Meurer et al., 1996). The mutant was unable to grow photoautotrophically but could be maintained on sucrose-supplemented agar medium. It was able to initiate rudimentary inflorescences; however, no fertile flowers were finally developed. Chlorophyll fluorescence induction experiments revealed that the transfer of excitation energy from the antenna to the reaction center of photosystem II was almost completely abolished and that the photochemical activity of the reaction center itself was severely impaired. P700 absorption measurements supported the chlorophyll fluorescence analyses by showing that the electron flow to photosystem I is inhibited (see Figure 3 and Table 2 in Meurer et al., 1996).

To substantiate and expand upon these findings, photosynthetic electron transport rates were measured. Three independent experiments showed that the photosystem II activity determined as light-induced electron transfer from H_2O to 2,5 dimethyl-*p*-benzoaminone (see Methods) was reduced to ~10 to 15% of the values for the wild-type level. Electron transport through photosystem I, that is, from tetramethyl-*p*-phenylene diamine to methylviologen, was also reduced but only by 40 to 50% when compared with that of the wild type. These findings corroborate the spectroscopic data by showing that both photosystems are affected although to varying degrees.

To learn more about the nature of the defect within the two photosystems, 77K fluorescence emission spectra were recorded. This technique permitted us to distinguish between characteristic emission bands of the chlorophyll–protein complexes CP43 and CP47 in photosystem II (688 and 695 nm) and the antenna of photosystem I (735 nm) (Krause and Weis, 1991; Krugh and Miles, 1995). Figure 1 shows that the two emission bands at 688 and 695 nm are absent in the mutant. These are replaced by a new single band at 685 nm, which is not

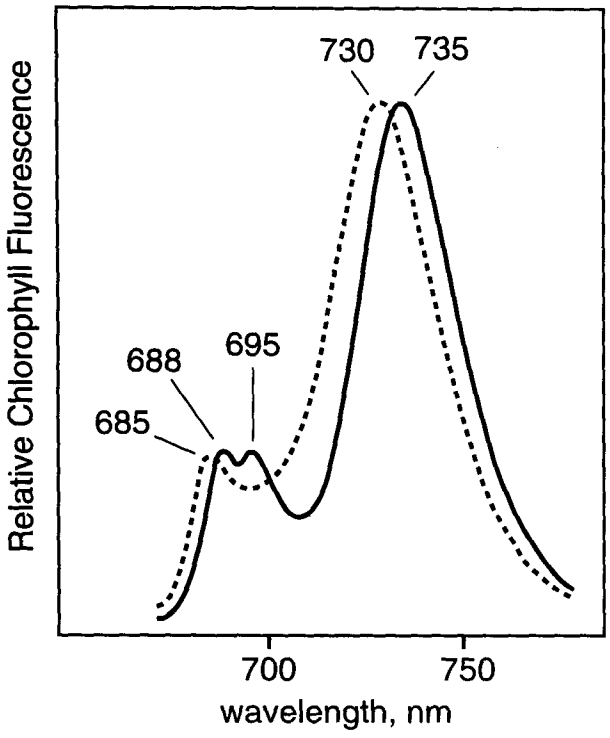

Figure 1. Chlorophyll Fluorescence Emission Spectra of *hcf109* and the Wild Type at 77K.

The spectra of *hcf109* (dashed line) and the wild type (solid line) show representative results of four measurements with independent plants.

found in the wild type. This additional band could arise from an increased fluorescence of the peripheral light-harvesting complex of photosystem II (LHCII) due to a reduced or inhibited transfer of exitons from LHCII to the inner antenna of that photosystem in *hcf109*. Although the band is usually slightly red-shifted from 682 to 685 nm, the deviation could be explained by the lack of the inner antenna, which results in a changed environment and consequently in an altered energetic characteristic of the outer antenna. These data confirm that the photosystem II complexes accumulating in the mutant are severely disturbed and appear to lack at least the functional inner antenna complexes CP43 and CP47.

A smaller difference was detected for the photosystem I–derived fluorescence band that shifts from 735 to 730 nm. Such a shift toward a shorter wavelength is typically observed when the outer antenna of photosystem I is impaired but the photosystem I core is almost intact. Its fluorescence emission band at 720 nm becomes more penetrating at the expense of the photosystem I antenna-derived signal (Krause and Weis, 1991). Taken together, the spectroscopic and photosynthetic electron transport measurements showed that *hcf109* is a pleiotropic mutant that affects both photosystem I and II functions. However, the larger alterations are associated with the function of the latter.

Photosystem I and II Polypeptides as well as Subunit H of NAD(P) Dehydrogenase Are Reduced in Mutant Thylakoids

To define the mutational defect more precisely, immunoblot experiments were performed using a collection of antisera that were raised against individual subunits of photosystems I and II, the cytochrome b_6f complex, the ATP synthase, and the plastid NAD(P)H dehydrogenase complex (see Table 1 in Meurer et al., 1996). Figure 2 shows that the thylakoid membranes of *hcf109* lost significant amounts of the constituent polypeptides of photosystems I and II. This explains the functional lesions that were detected in the spectroscopic and electron transport measurements. In addition, subunit H of the NAD(P)H dehydrogenase complex (NDHH) was substantially reduced, but the subunits of the cytochrome b_6f complex and ATP synthase accumulated to near wild-type levels.

When the levels of subunits A/B, C, D, and E of photosystem I (PSAA/B, PSAC, PSAD, and PSAE) were lowered, similar values were obtained, suggesting that photosystem I as a whole is diminished in the mutant. This could explain the reduction in the overall activity of this photosystem, which otherwise appears to function similar to the wild type (see above). However, the subunits of photosystem II did not show a concomitant reduction. The most reduced subunits were the inner antenna proteins CP47 and CP43 (PSBB and PSBC) and the reaction center polypeptides D1 and D2 (PSBA and PSBD). The levels of the other photosystem II polypeptides, that is, cytochrome b_{559} (PSBE/F), the 34- and 23-kD component of the oxygen-evolving complex (PSBO and PSBP), as well as the peripheral antenna proteins CP24 and CP29 (LHCB6 and LHCB4) were significantly less depleted (Figure 2). The nonstoichiometric amounts of photosystem II subunits suggest that truncated photosystem II complexes accumulate in *hcf109* and that they are likely to be functionally inactive and cause spectroscopic alterations, as detected by the chlorophyll fluorescence analyses.

To analyze the synthesis of photosystem I and II polypeptides, mutant and wild-type leaves were pulse-labeled with ^{35}S-methionine. The incorporation experiments were performed in the presence of cycloheximide, an inhibitor of cytoplasmic protein synthesis (Pestka, 1971), which reduces the complexity of the pattern of labeled proteins and allows easy identification of plastome-encoded polypeptides. After labeling, total soluble and membrane proteins were extracted, and equivalent amounts, based on the incorporated radioactive label, were analyzed on polyacrylamide–SDS gels prepared according to Schägger and von Jagow (1987). These gels provide excellent resolution, particularly in the low molecular weight range (Figures 3A and 3B), and allow a reliable identification of most major thylakoid membrane proteins without prior immunoprecipitation.

Figures 3A and 3B show that incorporation of label into PSAA/B, CP47, the mature form of D1, and a 5-kD thylakoid protein of unknown identity was significantly lowered in the

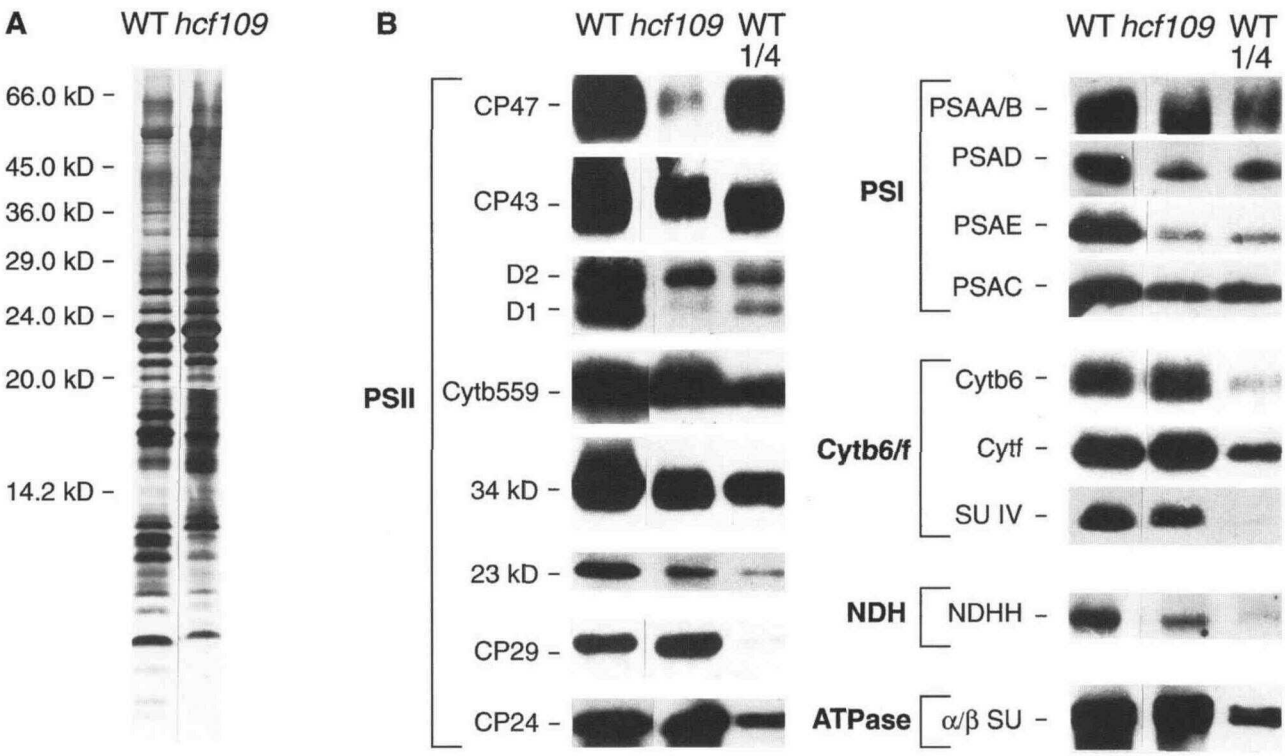

Figure 2. Gel Electrophoretic and Immunoblot Analysis of Mutant and Wild-Type Thylakoids.

(A) Thylakoid membrane polypeptides of mutant (*hcf109*) and wild-type (WT) thylakoids after electrophoresis on a 16% polyacrylamide–SDS gel and silver staining. Each lane contains thylakoid preparations corresponding to 8 μg of protein. The molecular masses (given in kD at the left of the panel) were estimated by coelectrophoresis with commercially available size standards (Dalton Mark VII-L; Sigma, Deisenhofen, Germany; RPN755, Amersham Buchler, Braunschweig, Germany).

(B) Composite fluorograph of an immunoblot analysis of mutant (*hcf109*) and wild-type (WT) thylakoids. Wild-type thylakoids equivalent to 8 (WT) or 2 μg (WT 1/4) of protein and mutant thylakoids (*hcf109*, 8 μg of protein) were electrophoresed on 16% polyacrylamide–SDS gels and immunodecorated with antisera, as described by Meurer et al. (1996). The immunoblots show representative results of three independent cultivations of plants. Thylakoid proteins analyzed are as follows: photosystem I (PSI), subunits PSAA/B (the P700 chlorophyll *a* apoproteins), PSAD, PSAE, and PSAC (the Fe-S subunit); photosystem II (PSII), CP47 and CP43 (the chlorophyll *a* apoproteins of the inner antenna), D1 and D2 (the P680-binding reaction center proteins), Cytb559 (cytochrome b_{559}), 34 and 23 kD (the 34- and 23-kD regulatory proteins of the oxygen evolving complex), CP29 and CP24 (light-harvesting complexes of the peripheral antenna); *cytochrome b_6f complex* (Cytb6/f), *cytochrome b_6* (Cytb6), *cytochrome f* (Cytf), and subunit 4 (SU IV); NAD(P)H dehydrogenase complex (NDH), subunit H (NDHH); and ATP synthase (ATPase), α and β subunits (α/β SU).

mutant. In contrast, the other thylakoid membrane proteins, among them CP43 as well as the soluble proteins (data not shown), incorporated similar amounts of ^{35}S-methionine in mutant and wild-type leaves (Figures 3A and 3B). Because the level of the CP43 protein is substantially reduced in the mutant (cf. Figures 2 and 3), whereas the incorporation of label into this protein is not, these data suggest that newly synthesized CP43 polypeptides are unstable and degrade rapidly (cf. Jensen et al., 1986; de Vitry et al., 1989). No clearcut data were obtained for the D2 polypeptide. This protein comigrated with the precursor of D1 (Figure 3A), and visual comparison of the autoradiographs did not permit an unequivocal distinction between these two proteins. Incorporation data are also lacking for subunit H of the NAD(P)H dehydrogenase and subunit C of photosystem I because no labeled bands of the expected molecular sizes (46 and 9 kD, respectively) could be detected. Taken collectively, the protein labeling experiments indicate that the *hcf109* mutation specifically affects the expression of several plastome-encoded photosystem I and II genes.

The Plastid *psbB*, *psbD/C*, *ndhC*, and *ndhH* Operons Are Deficient in Accumulating Distinct Transcripts

To investigate whether the mutational lesion of *hcf109* affects the accumulation of RNAs for components of the photosynthetic apparatus, RNA gel blots were prepared from total RNA and hybridized with a set of probes that cover both nuclear- and plastome-encoded transcripts (see Table 1).

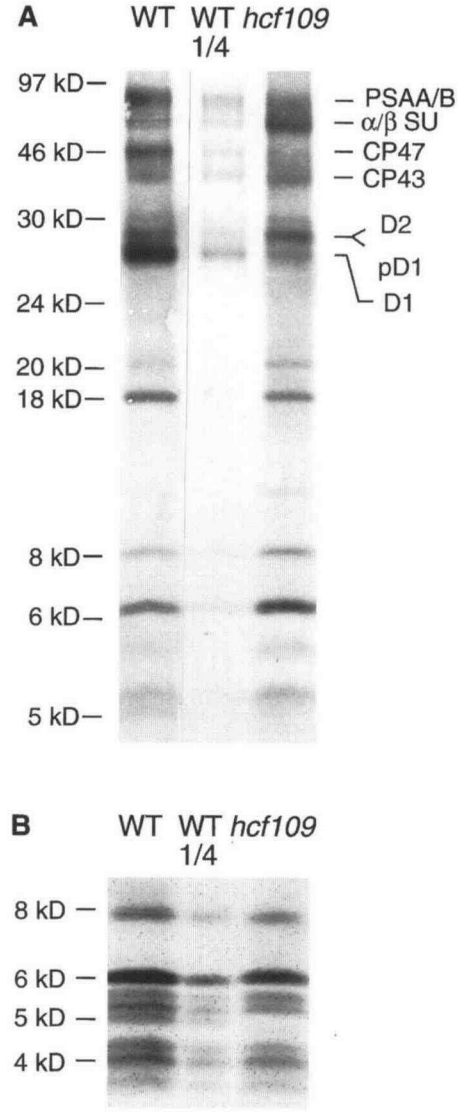

Figure 3. In Vivo Protein Synthesis with Primary Leaves of 12-Day-Old Mutant and Wild-Type Seedlings.

Incorporation of ^{35}S-methionine in the presence of cycloheximide was performed as described in Methods. Wild-type (WT) and mutant proteins with equivalent amounts of radioactivity (100,000 cpm [WT and *hcf109*] or 25,000 cpm [WT 1/4]) were loaded into each slot and electrophoresed on polyacrylamide–SDS gels. The separated proteins were transferred to a nitrocellulose membrane, and the ^{35}S label was visualized by autoradiography. To identify the labeled bands, the nitrocellulose filters containing the ^{35}S-labeled proteins were immunodecorated with antisera to PSAA/B, α and β subunits (α/β SU) of ATP synthase, CP47, CP43, D2, and D1 (data not shown). The molecular masses (given in kD) were estimated as described in the legend to Figure 2A.

(A) In vivo labeling pattern of thylakoid membrane proteins as determined by electrophoresis on a 10% polyacrylamide–SDS gel and subsequent autoradiography. For the labels of thylakoid proteins, see the legend to Figure 2B. pD1 denotes the precursor to the D1 polypeptide of the photosystem II reaction center.

Table 1. Plastome- and Nuclear-Encoded Genes Analyzed by RNA Gel Blot Hybridization[a]

Protein Complex/ Functional Unit	Plastome-Encoded Genes	Nuclear-Encoded Genes
Photosystem I	*psaA-psaB, psaC, psaI*	*psaD, psaF*
Photosystem II	*psbA, psbB-psbT, psbD-psbC, psbE-psbF-psbL-psbJ, psbH, psbI-psbK, psbN*	*psbO, psbP*
Cytochrome b_6f complex	*petA, petB-petD*	*petC*
NAD(P)H dehydrogenase	*ndhK, ndhJ, ndhH, ndhA, ndhI*	
ATP synthase	*atpA*	
Ribulose bisphosphate carboxylase	*rbcL*	*rbcS*
Transcriptional apparatus	*rpoA*	
Translational apparatus	*rps14, trnfM,* $trnG_{GCC}$, $trnG_{UCC}$, $trnR_{UCU}$, $trnS_{UGA}$	
Miscellaneous	*accD, cemA, ycf4, ycf9*	

[a] For details regarding the probes, see Meurer et al. (1996) and Methods.

Neither the steady state levels nor the sizes of RNAs were different in the mutant and wild type when blots were hybridized with probes for nuclear-encoded photosynthesis genes (see Table 1; data not shown). This result indicates that RNA accumulation for these selected nuclear genes was not altered in *hcf109*.

Identical transcript patterns and accumulation in the wild type and mutant were also observed for some plastome-encoded genes. These genes included *psbA* (encoding the D1 polypeptide of photosystem II), *psaA/B* (encoding subunits A and B of photosystem I), *rpoA* (encoding subunit A of the plastid RNA polymerase), *atpA* (encoding the α subunit of ATP synthase), *rbcL* (encoding the large subunit of ribulose bisphosphate carboxylase), and *petA* (encoding cytochrome *f*) (Figures 4A and 4B; data not shown). Whereas *psbA* and *rbcL* are transcribed monocistronically, all of the other genes are parts of polycistronic transcription units that, with the exception of *psaA/B*, are transcribed into complex RNA patterns. However, pronounced differences became apparent when

(B) In vivo labeling pattern of low molecular mass thylakoid membrane proteins, as determined by electrophoresis on a 16% polyacrylamide–SDS gel and subsequent autoradiography.

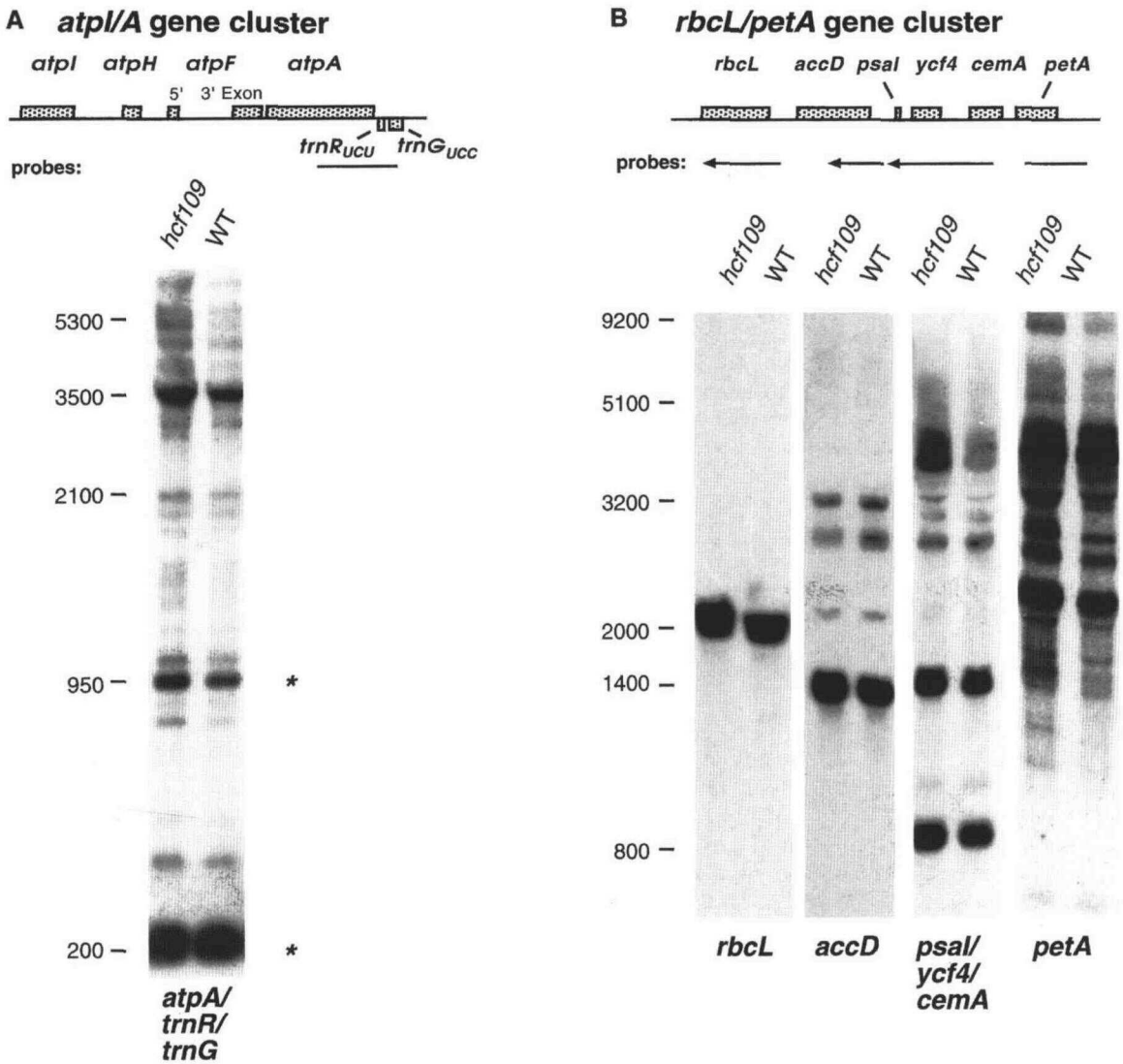

Figure 4. RNA Gel Blot Analysis of the Plastid *atpI/A* and *rbcL/petA* Gene Clusters in *hcf109* and the Wild Type.

The genetic composition of the operons and the locations of probes used for hybridization are illustrated at the top of the transcript patterns. Probes labeled by random oligonucleotide priming are shown as bars, whereas strand-specific hybridization probes generated by in vitro transcription are shown as arrows. Each lane contains 8 μg of total leaf RNA that was isolated from 3-week-old mutant (*hcf109*) and wild-type (WT) seedlings that had been grown on sucrose-supplemented agar medium. The numbers at the left indicate RNA sizes (given in nucleotides) that were estimated by coelectrophoresis with glyoxylated EcoRI/HindIII fragments of lambda DNA.

(A) RNA gel blot analysis of the *atpI/A* operon. *atpI*, *atpH*, and *atpF* encode subunits 4, 3, and 1 of the CF_0 part of ATP synthase, respectively, and *atpA* encodes the α subunit of the CF_1 part of ATP synthase. The positions of the tRNA genes $trnR_{UCU}$ and $trnG_{UCC}$, which are located 3' to *atpA*, are indicated. The coding sequences for these two tRNA genes are contained within the *atpA* hybridization probe. Because this probe has been labeled by random oligonucleotide priming, it will also hybridize to the mature tRNAs and their polycistronic precursors (labeled by asterisks).

(B) RNA gel blot analysis of the *rbcL/petA* gene cluster. *rbcL* encodes the large subunit of ribulose bisphosphate carboxylase; *accD*, a subunit of acetyl–coenzyme A carboxylase; *psaI*, the I subunit of photosystem I; *ycf4*, an unidentified open reading frame; *cemA*, a protein of the inner envelope whose function has not been resolved; and *petA*, cytochrome *f*.

analyzing the *psbB*, *psbD/C*, *ndhH*, and *ndhC* transcription units (Figures 5A to 5D). This result suggests that the *hcf109* gene product specifically affects the accumulation of plastome-encoded RNAs.

The *psbB* operon encodes the three photosystem II genes *psbB*, *psbT*, and *psbH* and the two cytochrome b_6f complex genes *petB* and *petD* (Barkan, 1988; Westhoff and Herrmann, 1988; Monod et al., 1994). Figure 5A shows that the levels of all transcripts carrying *psbB* coding sequences, that is, the polycistronic transcripts of 4.8 and 4.1 kb and the bicistronic *psbB-psbT* transcripts of 2.5, 2.1, and 1.9 kb, were drastically lowered. There was also a substantial reduction in the abundance of the primary polycistronic transcript of 5.7 kb. In contrast, the oligocistronic and monocistronic *petB* and *petD* transcripts of 2.6, 2.4, 1.55, 0.85, and 0.75 kb accumulated to wild-type levels. Wild-type levels were also observed for the monocistronic 0.40-kb *psbH* RNA. However, in the mutant, one additional *psbH*-containing transcript of 0.45 kb could be detected. The expression of *psbN*, which is located between *psbT* and *psbH* but transcribed in the opposite direction (Kohchi et al., 1988), was the same for both the mutant and the wild type.

Depletion of distinct transcripts was also observed in the *psbD/C* operon. In dicots, this operon is known to encode the two photosystem II genes *psbD* and *psbC*, the unidentified open reading frame *ycf9*, and perhaps $trnG_{GCC}$ (Offermann, 1988; Yao et al., 1989). Two promoters, one in front of *psbD* and one within its coding region, drive the transcription of this operon. Two processing sites located downstream of the two promoters produce additional RNA 5′ ends (Gamble et al., 1988; Yao et al., 1989; Christopher et al., 1992). At least one more processing site located behind *psbC* removes the *ycf9* part from the *psbD/C* segment (Berends et al., 1987).

Figure 5B shows that all *ycf9*-containing transcripts of 3.8, 3.3, 2.9, 2.2, and 2.0 kb are depleted, whereas the accumulation of the other RNAs of this operon, that is, the 3.3-, 2.9-, 2.6-, 1.8-, and 1.7-kb RNAs, was not affected by the mutation. As for the *psbB* transcription unit, the level of the primary polycistronic transcript (4.2 kb) of the *psbD-psbC-ycf9* operon was also reduced but not as much as the other *ycf9*-containing RNAs.

Drastic alterations in the transcript patterns were also apparent for two polycistronic transcription units that encode subunits of the plastid NAD(P)H dehydrogenase complex. The *ndhC* operon contains three *ndh* genes (*ndhC*, *ndhK*, and *ndhJ*), which are transcribed into a tricistronic *ndhC-ndhK-ndhJ* RNA of 2.1 kb and a dicistronic *ndhK-ndhJ* transcript of 1.7 kb (Steinmüller et al., 1989). It is not known whether both transcripts arise by transcriptional initiation or whether the latter is due to RNA processing. Figure 5C shows that *hcf109* seedlings are unable to accumulate any transcript of this transcription unit.

The *ndhH* transcription unit is characterized by a complex transcript pattern, which has been studied only by RNA blot hybridization (Matsubayashi et al., 1987; Kubicki et al., 1996). The polycistronic transcripts extend from *ndhH* to *ndhD* and demonstrate that this gene cluster represents a single transcriptional unit (Kubicki et al., 1996). However, no RNA 5′ and 3′ mapping or 5′ capping experiments have been conducted; therefore, RNA processing or additional internal transcription initiation sites are not known. Figure 5D shows that polycistronic transcripts of 6.8, 5.7, 5.0, and 3.9 kb are severely depleted in *hcf109*, whereas transcripts of intermediate sizes, that is, 3.2, 2.2, 1.75, and 1.2 kb, accumulated to wild-type levels. The most dramatic reduction was observed for the monocistronic 0.5-kb *psaC* RNA, suggesting that the mutational defect targets this segment of the operon. Interestingly, there is a transcript of 4.7 kb that accumulates in the mutant but is hardly detectable in the wild type.

We conclude that *hcf109* is severely disturbed in the transcript patterns of several but not all plastid polycistronic transcription units. In all affected transcription units, with the exception of the *ndhC* operon, only distinct transcripts do not accumulate, whereas the remainder are present at wild-type levels.

Run-On Analysis of Plastid Transcriptional Activity

To determine whether transcriptional or post-transcriptional processes are the major cause for the altered patterns of RNA accumulation, a run-on transcription system (Deng et al., 1987; Mullet and Klein, 1987) was established for Arabidopsis chloroplasts. In general, mutant and wild-type chloroplasts showed similar transcriptional activities (data not shown). Hybridization of radiolabeled run-on transcripts to membrane-bound, gene-specific antisense probes revealed no significant differences in the transcriptional activities of the *psbA*, *rbcL*, *psaA*, *psbB*, *petB/D*, *psbD/C*, *ycf9*, *psaC*, and *ndhK* genes (Figure 6). Thus, depletion of the *psbB*-, *ycf9*-, *psaC*-, and *ndhK*-containing transcripts in *hcf109* may not be linked with corresponding alterations in the transcription rates of these genes. It follows that post-transcriptional processes via the regulation of RNA stability must account for the differences in steady state RNA levels.

Molecular Mapping of the *hcf109* Locus

As an initial step toward the molecular characterization of the *hcf109* locus within the Arabidopsis genome, restriction fragment length polymorphism (RFLP) and polymerase chain reaction (PCR)–based marker mapping were used. With the ARMS RFLP marker set (Fabri and Schäffner, 1994), *hcf109* was located on chromosome 5 between markers 291C and 247A (Table 2). For more precise mapping of the *hcf109* locus, two microsatellite markers *nga76* and *nga139* (Bell and Ecker, 1994) and a cleaved amplified polymorphic sequence marker for the phytochrome C gene (*phyC*) (*Arabidopsis thaliana* Database, Stanford University, Stanford, CA) were used. Table 2 shows that the analysis of 1000 meiotic chromosomes did not result

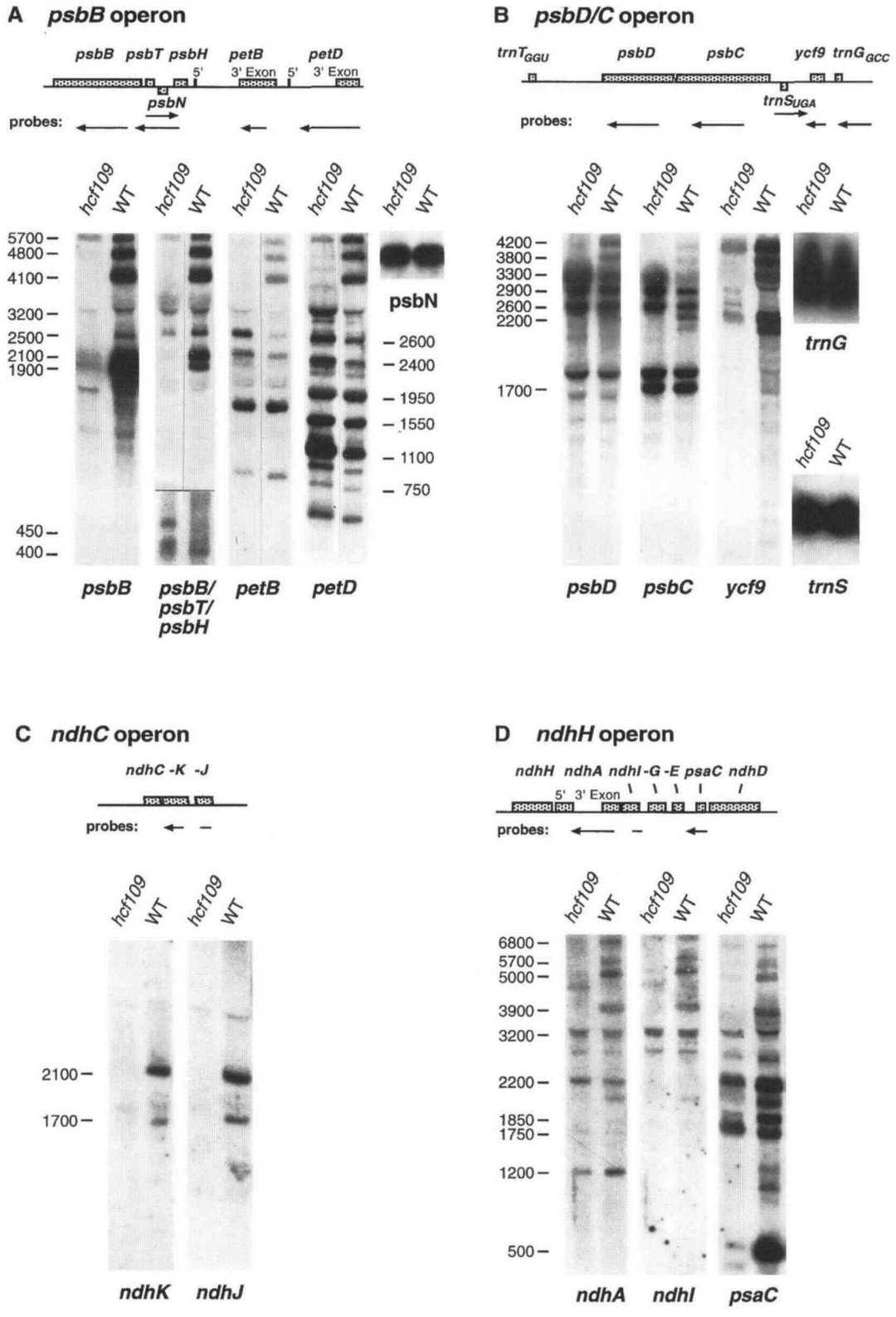

Figure 5. RNA Gel Blot Analysis of the Plastid *psbB*, *psbD/C*, *ndhC*, and *ndhH* Operons in *hcf109* and Wild-Type Plants.

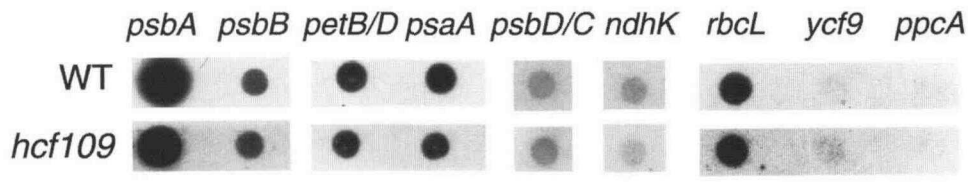

Figure 6. Run-On Analysis of the Transcriptional Activities of Several Plastid Genes in *hcf109* and the Wild Type.

The run-on transcripts of 5 × 10^6 chloroplasts from the wild type (WT) and *hcf109* were hybridized to immobilized gene-specific probes for *psbA*, *psbB*, *petB/D*, *psaA*, *psbD/C*, *ndhK*, *rbcL*, and *ycf9* (see Table 1 and Meurer et al. [1996] for probe details). A cDNA for the nuclear-encoded *ppcA* gene of *F. trinervia* (Poetsch et al., 1991) was used as a control for background hybridization. The bound radioactivity was visualized by autoradiography; a representative of four independent experiments is shown here. The hybridized run-on transcripts were also quantitated by liquid scintillation counting. When the relative transcription rates of *psbA* in *hcf109* and the wild type were arbitrarily set to 100 and used to normalize the transcription activities of the other genes, the following mean values of four independent experiments were obtained: *psbB*: WT, 2.5 ± 0.5, *hcf109*, 3.4 ± 0.8; *petB/D*: WT, 4.1 ± 0.3, *hcf109*, 4.6 ± 0.5; *psaA*: WT, 3.6 ± 0.2, *hcf109*, 4.3 ± 0.8; and *rbcL*: WT, 7.9 ± 1.0, *hcf109*, 11.3 ± 1.2. The hybridization signals obtained with the *psbD/C*, *ndhK*, and *ycf9* probes were close to background hybridization (*ppcA*) and are not included here.

in any recombination event between *hcf109* and *phyC*. Thus, *hcf109* must be <0.1 centimorgans apart from *phyC*, which should be in the range of ~20 kb.

DISCUSSION

Conclusive evidence from various genetic and biochemical studies (Rochaix, 1992; Barkan et al., 1995; Mayfield et al., 1995) indicates that plastid gene expression is controlled by the activities of a large number of nuclear-encoded genes. It is reasonable to expect that most of the regulatory factors encoded by these genes will represent minority factors. A combined genetic and molecular biological approach is therefore likely to be the method of choice for identifying these controlling genes and for dissecting the regulatory network in which they are involved. Here, we describe a nuclear high-chlorophyll fluorescence mutant of Arabidopsis. This mutant is impaired by the accumulation of distinct transcripts from four different transcription units.

Phenotypically, *hcf109* can be classified as a pleiotropic mutant whose photosynthetic electron transport chain is almost totally inactive due to defects in photosystems I and II and the plastid NAD(P)H dehydrogenase complex. Immunoblot analysis indicated the absence of defects in the cytochrome b_6f complex and ATP synthase. Electron transport measurements and various spectroscopic techniques were used to define as precisely as possible the lesions within the two photosystems. No attempts were made to probe into the NAD(P)H dehydrogenase, because neither an unambiguous assay system nor specific inhibitors were available to test for this thylakoid membrane complex.

Chlorophyll fluorescence induction kinetics (Meurer et al., 1996) and electron transport measurements showed that *hcf109* is severely impaired in light-induced electron transport through photosystem II. The 77K fluorescence spectra support these results by pointing to the inner antenna complex as the putative target of the primary lesion within this photosystem. The drastic reduction of photosystem II–driven electron flow is also reflected in the absorption kinetics of P_{700}. Oxidized P_{700} may be reduced only partially by illumination with a strong white light pulse (Meurer et al., 1996), although substantial amounts of functional photosystem I reaction center do exist in *hcf109*. However, linear electron transport from photosystem II via the cytochrome b_6f complex is not the sole provider of electrons to photosystem I. In addition, a cyclic electron flow exists around photosystem I (Bendall and Manasse, 1995), which may receive

Figure 5. (continued).

For experimental details, see the legend to Figure 4. WT, wild type.

(A) RNA gel blot analysis of the *psbB* operon. *psbB* encodes the CP47 chlorophyll *a* apoprotein of photosystem II; *psbT*, a 4-kD subunit; *psbH*, the 10-kD phosphoprotein subunit; and *psbN*, another 4-kD subunit. *petB* and *petD* encode subunits cytochrome b_6 and IV, respectively, of the cytochrome b_6f complex. The lower part of the filter hybridized with antisense transcripts to *psbB/psbT/psbH* was overexposed to increase the signal of the monocistronic *psbH* band.

(B) RNA gel blot analysis of the *psbD/C* operon. *psbD* and *psbC* encode the D2 polypeptide and the CP43 chlorophyll *a* apoprotein of photosystem II, respectively; *ycf9*, an unidentified open reading frame; and $trnT_{GGU}$, $trnG_{GCC}$, and $trnS_{UGA}$, tRNAs for threonine, glycine, and serine, respectively.

(C) RNA gel blot analysis of the *ndhC* operon. *ndhC*, *ndhK*, and *ndhJ* encode the corresponding subunits of the plastid NADP(H) dehydrogenase complex.

(D) RNA gel blot analysis of the *ndhH* operon. *ndhH*, *ndhA*, *ndhI*, *ndhG*, *ndhE*, and *ndhD* encode the corresponding subunits of the plastid NADP(H) dehydrogenase complex; *psaC*, subunit C of photosystem I.

Table 2. Mapping Data for *hcf109*[a]

Marker	Chromosomes Analyzed	Percentage of Recombination	Genetic Distance (in centimorgans)	LOD Score[b]
291C	38	15.8 ± 4.2	16.4 ± 4.7	4.2
247A	42	4.8 ± 2.3	4.8 ± 2.3	9.2
nga139	110	20.0 ± 2.7	21.2 ± 3.2	9.2
nga76	280	4.3 ± 0.9	4.3 ± 0.9	62.8
phyC[c]	1000	<0.1 ± 0.07	<0.1 ± 0.07	>300

[a] For experimental details, see Methods.
[b] Logarithm of the likelihood odd ratio supporting linkage between *hcf109* and the marker.
[c] No recombination event between *phyC* and *hcf109* was detected.

electrons from the NAD(P)H dehydrogenase complex (Kubicki et al., 1996). Because *hcf109* is deficient in the NAD(P)H dehydrogenase, this lesion may contribute to the almost complete lack of electron flow into photosystem I.

The impaired functions of photosystems I and II are mirrored at the protein and RNA levels. Immunoblot analyses demonstrated that all of the analyzed photosystem I subunits are reduced by ~75%. Although the *psaA*–psaB transcripts accumulated to wild-type levels in *hcf109*, there was a drastic reduction in the steady state amounts of the monocistronic *psaC* RNA. Limiting amounts of this RNA may explain the diminished numbers of photosystem I complexes, because it is known from mutational analysis with Chlamydomonas that the *psaC* product is essential for the correct assembly of this photosystem (Takahashi et al., 1991).

The accumulation of all analyzed photosystem I subunits in *hcf109* was lowered by similar values. In contrast, photosystem II polypeptides accumulated nonstoichiometrically. This result agrees with observations of photosystem II mutants of Chlamydomonas (de Vitry et al., 1989), the greening of etiolated spinach seedlings (Westhoff et al., 1990), and bundle sheath chloroplasts of monocotyledonous C_4 plants (Meierhoff and Westhoff, 1993). The highest reductions of the amount of protein and the incorporation of ^{35}S-methionine in in vivo labeling experiments were observed for CP47 and D1. Such a coordinated synthesis and concomitant accumulation of CP47 and D1 have also been found in CP47 mutants of Chlamydomonas (Jensen et al., 1986; Monod et al., 1992) and Synechocystis (Shen et al., 1993).

The lowered level and synthesis of CP47 were paralleled by a depletion of the amount of *psbB*-containing transcripts, indicating a causal relationship. In contrast, the levels of *psbA* and other plastome-encoded photosystem II transcripts were not changed in *hcf109*, and accumulation of corresponding proteins was reduced. These findings suggest that the limiting amounts of CP47 are the primary cause for the deficiency in photosystem II and that the reduced levels of the other photosystem II subunits are a secondary effect. Because *psbT* sequences are always carried on the same transcripts as *psbB*, a concomitant loss of the *psbT* protein may contribute to the observed photosystem II phenotype. However, this appears unlikely because the inactivation of *psbT* in Chlamydomonas did not cause any disturbances in photosystem II under normal growth conditions (Monod et al., 1994).

Besides the severe depletion in *psbB–psbT* transcripts, *hcf109* also lacks all *ycf9*-containing transcripts. The *ycf9* reading frame is not found on a separate RNA but always occurs together with *psbD* and *psbC* sequences. The function of the YCF9 protein has not been elucidated, and it is not known whether the co-location of *ycf9*, *psbD*, and *psbC* sequences on the same RNAs implies any functional relationship. The drastic depletion of *ycf9* transcripts in the photosystem II–depleted bundle sheath chloroplasts of monocotyledonous NADP malic enzyme–type C_4 species (Westhoff et al., 1991; Kubicki et al., 1994) may suggest a functional association of *ycf9* with this photosystem.

The most intriguing feature of *hcf109* is that the mutational lesion impairs RNA accumulation in four different polycistronic transcription units but only distinct transcripts in the multibanded pattern of the *psbB*, *psbD/C*, and *ndhC* operons are lacking. Because transcriptional run-on experiments revealed no significant differences in the transcriptional activities of the corresponding genes, the mutation must affect RNA accumulation at the level of transcript stability and not of transcription initiation. An *hcf* locus (*hcf38*) that affects the accumulation of *psbB* transcripts has also been described in maize (Barkan et al., 1986). In addition, the locus affects RNA accumulation in the *petA* and *atpB/E* gene clusters and is therefore different from the *hcf109* gene of Arabidopsis.

The pleiotropic effects of the two *hcf* loci of Arabidopsis and maize on RNA accumulation in several polycistronic transcription units contrast with our current knowledge about nuclear mutations affecting plastid mRNA stability in Chlamydomonas. All mutations that have been identified are specific and affect only individual mRNAs, for instance, those encoding *psbB* (Sieburth et al., 1991; Monod et al., 1992), *psbC* (Sieburth et al., 1991), or *psbD* transcripts (Kuchka et al., 1989). The limited available data do not permit any conclusions about this discrepancy between land plants and Chlamydomonas. However, the two plastomes differ widely with respect to genome organization (Palmer, 1992); perhaps even more importantly, land plants and chlorophycean algae are derived from independent lineages that separated at the beginning of the evolution of the chlorophyll *a/b*–containing plants (Steinkötter et al., 1994). It is to be expected that significant differences in the regulation of plastid gene expression in these two lineages of chlorophyll *a/b*–containing photosynthetic eukaryotes have evolved.

For the mechanism of action of the *hcf109* gene product, two principal modes may be envisioned. Due to the recessive nature of the mutation, the mechanism could act as a negative regulator of a specific nuclease or processing activity that renders the transcripts more susceptible to degradation. This could be an RNA binding protein which recognizes *cis*-acting

elements in the *psbB-psbT, ycf9, psaC,* and *ndhC/K/J* transcripts and thereby confers stability on these RNAs. Alternatively, it might not contact RNA directly but might represent a component of a multimeric complex. In any case, one would expect that sequence motifs and/or structures that provide recognition sites for the *hcf109* gene product or its associated components are common to all of the above transcripts. The transcribed sequences of the *psbB-psbT, ycf9, psaC,* and *ndhC/ndhK/ndhJ* genes and adjacent regions were examined visually and by computer-aided searches to identify eventually those *cis*-regulatory sequence motifs. No particularly convincing sequence similarities were detected in the 3′ flanking regions of *psbT, ycf9, ndhJ,* and *psaC.* This contrasts with a conserved hexanucleotide motif (CCAATG) that can be found 5′ upstream of *psbB, ycf9,* and *ndhk* and just at the translational start codon of *psaC* (Figure 7). Its significance may be questioned, however; in the case of *psbB* (Westhoff and Herrmann, 1988) and *ycf9* (Offermann, 1988), it has been shown that the corresponding RNA segment contains an endonucleolytic processing site (see Figure 7). Cleavage at this site leads to the formation of a 5′ truncated version of the *psbB–psbT* dicistronic RNA (Westhoff and Herrmann, 1988) and to the removal of the *ycf9* region from the *psbD–psbC* transcript segment, respectively (Offermann, 1988). Unfortunately, no 5′ mapping data are available for the monocistronic *psaC* RNA and the dicistronic *ndhK–ndhJ* transcript. For this reason, there is still no evidence that these CCAATG-containing regions are the target site of the *hcf109* gene product.

The importance of the 5′ leader segment for RNA stability is well documented for mitochondrial transcripts in yeast (Dieckmann et al., 1984; Chen and Dieckmann, 1994; Grivell, 1995) and also for the *psbD* transcript in the chloroplasts of Chlamydomonas (Kuchka et al., 1989; Nickelsen et al., 1994). Similar data for plastid RNAs of higher plants are lacking. It is hoped that the isolation and molecular characterization of the *hcf109* locus will shed new light on the regulation of plastid RNA stability by transcript-specific proteins. The proximity of the *hcf109* locus to the *phyC* gene should permit a successful isolation of *hcf109* by positional cloning and provide this important information in the near future.

METHODS

Plant Material and Growth Conditions

Seeds of *Arabidopsis thaliana* ecotypes Columbia and Landsberg *erecta* were obtained from J. Dangl (formerly of Max-Delbrück Laboratory, Max-Planck-Institut für Züchtungsforschung, Cologne, Germany). Both mutant and wild-type plants were grown on sucrose-supplemented Gelrite medium (Meurer et al., 1996). All comparisons between mutant and wild type were performed with leaf material at the same developmental stage.

Photosynthetic Electron Transport Measurements

Thylakoid membranes were isolated by homogenizing 1- to 2-g leaves from 24-day-old mutant and wild-type seedlings in 20 mL of 20 mM Tricine-KOH, pH 8, 10 mM NaCl, and 400 mM sucrose, using a Waring blender. Following filtration through 20-μm nylon cloth, the membranes were centrifuged for 10 min at 4500 rpm (HB-4 rotor; Sorvall-Dupont, Bad Nauheim, Germany), washed in the same buffer, and finally suspended in 20 mM Tricine-KOH, pH 8, 150 mM NaCl, and 5 mM $MgCl_2$. The chlorophyll content was determined according to Arnon (1949). Polarographic measurements of the light-driven activities of photosystems I and II were conducted by using a homemade oxygen electrode (Delieu and Walker, 1972) in saturating light at 20°C. Photosystem I–dependent electron transport was measured in the presence of 1 μM 3-[3,4-dichlorophenyl]-1,1-dimethylurea by using 0.5 mM *N,N,N′,N′*-tetramethyl-*p*-phenylendiamine, which was reduced with 0.5 mM sodium ascorbate as electron donor and 25 μM methyl viologen as electron acceptor. The reaction medium contained additional 40 mM Tricine-KOH, pH 8.0, 60 mM KCl, and 5 mM $MgCl_2$ (Allen and Holmes, 1986). Photosystem II–mediated oxygen evolution was measured by using 2,5-dimethyl-*p*-benzoaminone as electron acceptor in a medium containing 330 mM sorbitol, 5 mM $MgCl_2$, 5 mM NaCl, 1 mM KH_2PO_4, and 40 mM Hepes-KOH, pH 7.6 (Somersalo and Krause, 1990).

Low-Temperature Chlorophyll Fluorescence Spectra

Chlorophyll fluorescence emission spectra at 77K were recorded for primary leaves of 16-day-old plants with a fluorometer (model F-3010;

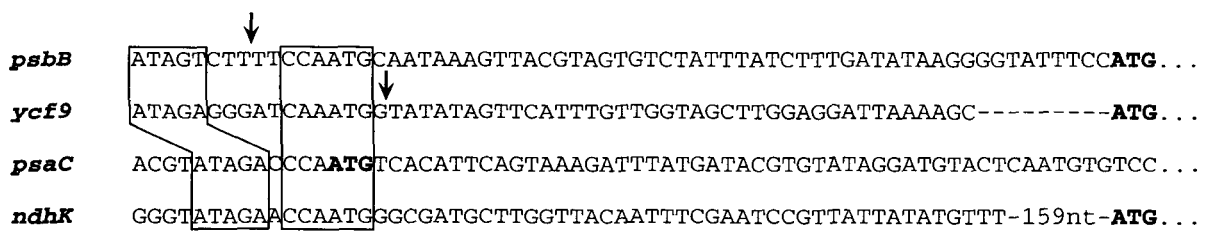

Figure 7. Alignment of Sequences in the 5′-Leader and Coding Regions of *psbB, ycf9, psaC,* and *ndhK.*

Sequences were taken from tobacco plastid DNA (Shinozaki et al., 1986). Vertical arrows denote RNA 5′ ends as determined by S1 nuclease protection analysis with spinach (Westhoff, 1985; Offermann, 1988). The conserved hexanucleotide motif CCAATG and the pentanucleotide motif ATAGA are boxed. The translational initiation codons are written in boldface letters. The *ndhK* upstream region is actually located within *ndhC* (Steinmüller et al., 1989).

Hitachi, Tokyo, Japan), as described by Weis (1985). Fluorescence was excited at 475 nm (band pass 20 nm), and the emission was recorded between 670 and 780 nm (band pass 1.5 nm). Emission spectra from 25 single measurements were averaged, and the emission maxima were determined by calculating the second order derivative spectra with a personal computer. Spectra were normalized with respect to equivalent long wavelength emission bands.

In Vivo Labeling of Leaf Proteins

Primary leaves of 12-day-old mutant and wild-type seedlings were vacuum infiltrated in 50-μL reaction medium containing 1 mM KH_2PO_4, pH 6.3, 0.1% (w/v) Tween 20, 50 μCi ^{35}S-methionine (specific activity >1000 Ci/mmol; Amersham Buchler, Braunschweig, Germany) and 20 μg/mL cycloheximide. After a 15-min incubation at 25°C in ambient light, leaves were washed twice with 500 μL of 20 mM Na_2CO_3 and 10 mM DTT. Thylakoid membranes were isolated from leaves after grinding with a conical stainless steel rod that fitted into the bottom of an Eppendorf tube. The homogenate was centrifuged for 10 min at 15,000 rpm (2MK centrifuge; Sigma, Osterode, Germany). The pellet with the membranes was washed and resuspended in 100 mM Na_2CO_3, 10% (w/v) sucrose, and 50 mM DTT. Trichloroacetic acid–insoluble radioactivity was measured according to Mans and Novelli (1961).

PAGE and Immunoblotting

Electrophoresis of proteins in SDS–polyacrylamide gels was performed according to Schägger and von Jagow (1987). Separated proteins were silver stained according to Blum et al. (1987). Radiolabeled proteins were detected by autoradiography after electrophoretic transfer to a nitrocellulose membrane. Proteins for immunodecoration analysis were also transferred to nitrocellulose membranes, incubated with specific antibodies (Westhoff et al., 1985), and visualized by the enhanced chemiluminescence Western blotting technique (Amersham Buchler) (Meurer et al., 1996).

RNA Gel Blotting

Gel blot analysis of total leaf RNA by using DNA or RNA probes was performed as described previously (Westhoff and Herrmann, 1988; Westhoff et al., 1991; Meurer et al., 1996). Hybridization probes for plastid- or nuclear-encoded RNAs are listed in Meurer et al. (1996) and Kubicki et al. (1996). Additional gene probes of spinach plastid DNA were pSoP930 (containing a 1041-bp XbaI fragment; P. Westhoff, unpublished data) for *rpoA*, pSoP3303 (containing a 1100-bp BamHI/EcoRI fragment; M. Streubel and P. Westhoff, unpublished data) for *accD*, and pSoP3034 (containing a 2100-bp EcoRI fragment; M. Streubel and P. Westhoff, unpublished data) for *psaI/ycf4/cemA*.

Run-On Transcription Reactions and Hybridization of Radiolabeled Run-On Transcripts to Membrane-Bound RNA Probes

Crude chloroplasts were isolated from 3 g of leaf material of 12-day-old mutant or wild-type seedlings, essentially as described by Somerville et al. (1981). Further purification of the chloroplasts on a Percoll step gradient (42%/85%) followed the protocol of Bartlett et al. (1982). Chloroplasts were resuspended in 300 mM sorbitol and 50 mM Hepes-NaOH, pH 8.0, and their concentration was determined in a hemocytometer. Run-on transcription assays with 5×10^6 chloroplasts per 55 μL of total reaction volume were performed as described by Klein and Mullet (1990) with the modifications listed in Kubicki et al. (1994). After 10 min of incubation at 25°C, transcription was terminated and the radiolabeled RNAs were isolated (Kubicki et al., 1994). Incorporation of α-^{32}P-UTP into transcripts was determined as described by Hallick et al. (1976).

Antisense transcripts to *psbA*, *psbB*, *psbD/C*, *petB/D*, *rbcL*, *psaA*, *ycf9*, and *ndhK* were produced by in vitro transcription, as described by Klein and Mullet (1990). Approximately 8 pmol of in vitro transcript was glyoxylated (McMaster and Carmichael, 1977) and immobilized onto Biodyne A nylon membranes (0.2 μm; Pall, Dreieich, Germany), using a Minifold I dot blot device (Schleicher & Schuell). Prehybridizations and hybridizations with ^{32}P-labeled run-on transcripts were performed according to Klein and Mullet (1990). To exclude competition of probes for the same polycistronic transcripts, the probes of one transcription unit were always assayed in separate hybridization reactions. Blots were analyzed by autoradiography and liquid scintillation counting of the excised spots.

Mapping of *hcf109*

Seventy-five F_2 populations were produced by pollinating emasculated flowers of the ecotype Landsberg *erecta* with Columbia plants heterozygous for the *hcf109* mutation and selfing the resulting F_1 plants. Twenty-two F_2 plants that were homozygous for the wild-type *hcf109* locus of Landsberg *erecta* were selected from the segregating F_2 populations and used to generate F_3 families for restriction fragment length polymorphism (RFLP) analysis. They were also used for polymerase chain reaction (PCR)–based marker typing; in addition, individual F_2 plants that were homozygous for the mutant locus were included in the analysis.

For RFLP mapping, DNA was isolated from ~60 plants of the F_3 families (Dellaporta et al., 1983). One microgram of EcoRI-digested DNA was separated in agarose gels and subjected to DNA gel blotting using standard procedures of Sambrook et al. (1989) and the ARMS marker set of Fabri and Schäffner (1994).

PCR analysis was performed with isolated genomic DNA (Dellaporta et al., 1983) or with a crude leaf homogenate (Klimyuk et al., 1993). The microsatellite markers *nga76* and *nga139* were amplified according to Bell and Ecker (1994). The primer for the cleaved amplified polymorphic sequence marker (Konieczny and Ausubel, 1993) of phytochrome C (*phyC*) was as follows: forward primer, 5′-CCTAATGGAGAATCATTCGG-3′; reverse primer, 5′-CTACAGAATCGTCCTCAACG-3′ (*Arabidopsis thaliana* Database). Amplification with the *phyC* primers yielded a product of ~2 kb, which, after digestion with PstI, resulted in 1.7- and 0.3-kb fragments for the Columbia allele and in 0.8-, 0.7-, 0.3-, and 0.2-kb fragments for the Landsberg *erecta* ecotype.

Chi square tests were used to assess genetic linkage of the *hcf109* locus with the RFLP markers. The relative map positions of *hcf109* and marker loci were determined with MapMaker 2.0 for Macintosh (Apple Computers, Inc., Cupertino, CA) (Lander et al., 1987) by using the Kosambi mapping function and a log-likelihood threshold of 4.0. Standard errors of recombination frequency and map distances were estimated according to Koornneef and Stam (1992).

ACKNOWLEDGMENTS

We thank Drs. Jeff Dangl (formerly of Max-Delbrück Laboratory, Max-Planck-Institut für Züchtungsforschung, Cologne, Germany), Toni Schäffner (Institut für Biochemie, Ludwig-Maximilians-Universität, Munich, Germany), and the Arabidopsis Biological Resource Center (Ohio State University, Columbus) for providing numerous clones and seeds. We are grateful to Dr. Uwe Santore (Institut für Entwicklungs- und Molekularbiologie der Pflanzen, Heinrich-Heine-Universität Düsseldorf) for comments on the English text and to other members of our laboratory for helpful suggestions and discussions. We also thank Dr. Hendrik Laasch (Institut für ökologische Pflanzenphysiologie und Geobotanik, Heinrich-Heine-Universität Düsseldorf) for help with the low-temperature fluorescence emission spectra. Grant support from the Deutsche Forschungsgemeinschaft through Sonderforschungsbereich 189 and the Fonds der Chemischen Industrie is gratefully acknowledged. Parts of this work have been submitted for the doctoral thesis of J.M.

Received February 27, 1996; accepted May 20, 1996.

REFERENCES

Allen, J.F., and Holmes, N.G. (1986). Electron transport and redox titration. In Photosynthesis: Energy Transduction: A Practical Approach, M.F. Hipkins and N.R. Baker, eds (Oxford: IRL Press), pp. 103–141.

Arnon, D.I. (1949). Copper enzymes in isolated chloroplasts: Polyphenoloxidase in *Beta vulgaris*. Plant Physiol. **24,** 1–13.

Båga, M., Göransson, M., Normark, S., and Uhlin, B.E. (1988). Processed mRNA with differential stability in the regulation of *E. coli* pilin gene expression. Cell **52,** 197–206.

Barkan, A. (1988). Proteins encoded by a complex chloroplast transcription unit are each translated from both monocistronic and polycistronic mRNAs. EMBO J. **7,** 2637–2644.

Barkan, A., Miles, D., and Taylor, W.C. (1986). Chloroplast gene expression in nuclear, photosynthetic mutants of maize. EMBO J. **5,** 1421–1427.

Barkan, A., Walker, M., Nolasco, M., and Johnson, D. (1994). A nuclear mutation in maize blocks the processing and translation of several chloroplast mRNAs and provides evidence for the differential translation of alternative mRNA forms. EMBO J. **13,** 3170–3181.

Barkan, A., Voelker, R., Mendel-Hartvig, J., Johnson, D., and Walker, M. (1995). Genetic analysis of chloroplast biogenesis in higher plants. Physiol. Plant. **93,** 163–170.

Bartlett, S.G., Grossman, A.R., and Chua, N.-H. (1982). In vitro synthesis and uptake of cytoplasmically synthesized chloroplast proteins. In Methods in Chloroplast Molecular Biology, M. Edelman, R. Hallick, and N.-H. Chua, eds (Amsterdam: Elsevier Biomedical Press), pp. 1081–1091.

Bell, C.J., and Ecker, J.R. (1994). Assignment of 30 microsatellite loci to the linkage map of Arabidopsis. Genomics **19,** 137–144.

Bendall, D.S., and Manasse, R.S. (1995). Cyclic photophosphorylation and electron transport. Biochim. Biophys. Acta **1229,** 23–38.

Berends, T., Gamble, P.E., and Mullet, J.E. (1987). Characterization of the barley chloroplast transcription units containing *psaA-psaB* and *psbD-psbC*. Nucleic Acids Res. **15,** 5217–5240.

Blowers, A.D., Klein, U., Ellmore, G.S., and Bogorad, L. (1993). Functional in vivo analyses of the 3′ flanking sequences of the Chlamydomonas chloroplast *rbcL* and *psaB* genes. Mol. Gen. Genet. **238,** 339–349.

Blum, H., Beier, H., and Gross, H.J. (1987). Improved silver staining of plant proteins, RNA and DNA in polyacrylamide gels. Electrophoresis **8,** 93–99.

Chen, C.Y.A., Beatty, J.T., Cohen, S.N., and Belasco, J.G. (1988). An intercistronic stem–loop structure functions as an mRNA decay terminator necessary but insufficient for *puf* mRNA stability. Cell **52,** 609–619.

Chen, H.C., and Stern, D.B. (1991). Specific ribonuclease activities in spinach chloroplasts promote mRNA maturation and degradation. J. Biol. Chem. **266,** 24205–24211.

Chen, W., and Dieckmann, C.L. (1994). *Cbp1p* is required for message stability following 5′ processing of COB mRNA. J. Biol. Chem. **269,** 16574–16578.

Christopher, D.A., Kim, M., and Mullet, J.E. (1992). A novel light-regulated promoter is conserved in cereal and dicot chloroplasts. Plant Cell **4,** 785–798.

Delieu, T., and Walker, D.A. (1972). An improved cathode for the measurement of photosynthetic oxygen evolution by isolated chloroplasts. New Phytol. **71,** 201–225.

Dellaporta, S.L., Wood, J., and Hicks, J.B. (1983). A plant DNA minipreparation: Version II. Plant Mol. Biol. Rep. **1,** 19–21.

Deng, X.-W., Stern, D.B., Tonkyn, J.C., and Gruissem, W. (1987). Plastid run-on transcription: Application to determine the transcriptional regulation of spinach plastid genes. J. Biol. Chem. **262,** 9641–9648.

de Vitry, C., Olive, J., Drapier, D., Recouvreur, M., and Wollman, F.-A. (1989). Posttranslational events leading to the assembly of photosystem II protein complex: A study using photosynthesis mutants from *Chlamydomonas reinhardtii*. J. Cell Biol. **109,** 991–1006.

Dieckmann, C.L., Koerner, T.J., and Tzagoloff, A. (1984). *CBP1*, a yeast gene involved in 5′ end processing of cytochrome *b* pre-mRNA. J. Biol. Chem. **259,** 4722–4731.

Douglas, S.E. (1994). Chloroplast origins and evolution. In The Molecular Biology of Cyanobacteria, D.A. Bryant, ed (Dordrecht, The Netherlands: Kluwer Academic Publishers), pp. 91–118.

Eddy, C.K., Keshav, K.F., An, H., Utt, E.A., Mejia, J.P., and Ingram, L.O. (1991). Segmental message stabilization as a mechanism for differential expression from the *Zymomonas mobilis gap* operon. J. Bacteriol. **173,** 245–254.

Fabri, C.O., and Schäffner, A.R. (1994). An *Arabidopsis thaliana* RFLP mapping set to localize mutations to chromosomal regions. Plant J. **5,** 149–156.

Gamble, P.E., Berends-Sexton, T., and Mullet, J.E. (1988). Light-dependent changes in *psbD* and *psbC* transcripts of barley chloroplasts: Accumulation of two transcripts maintains *psbD* and *psbC* translation capability in mature chloroplasts. EMBO J. **7,** 1289–1297.

Grivell, L.A. (1995). Nucleo–mitochondrial interactions in mitochondrial gene expression. Crit. Rev. Biochem. Mol. Biol. **30,** 121–164.

Gruissem, W., and Schuster, G. (1993). Control of mRNA degradation in organelles. In Control of Messenger RNA Stability, J.G. Belasco and G. Brawerman, eds (Orlando, FL: Academic Press), pp. 329–365.

Haley, J., and Bogorad, L. (1990). Alternative promoters are used for genes within maize chloroplast polycistronic transcription units. Plant Cell **2**, 323–333.

Hallick, R.B., Lipper, C., Richards, O.C., and Rutter, W.J. (1976). Isolation of a transcriptionally active chromosome from chloroplasts of *Euglena gracilis*. Biochemistry **15**, 3039–3045.

Herrmann, R.G., Westhoff, P., and Link, G. (1992). Biogenesis of plastids in higher plants. In Plant Gene Research: Cell Organelles, R.G. Herrmann, ed (Vienna: Springer-Verlag), pp. 275–349.

Hudson, G.S., Mason, J.G., Holton, T.A., Koller, B., Cox, G.B., Whitfeld, P.R., and Bottomley, W. (1987). A gene cluster in the spinach and pea chloroplast genomes encoding one CF_1 and three CF_0 subunits of the H^+-ATP synthase complex and the ribosomal protein S2. J. Mol. Biol. **196**, 283–298.

Jensen, K.H., Herrin, D.L., Plumley, F.G., and Schmidt, G.W. (1986). Biogenesis of photosystem II complexes: Transcriptional, translational, and posttranslational regulation. J. Cell Biol. **103**, 1315–1325.

Kapoor, S., Wakasugi, T., Deno, H., and Sugiura, M. (1994). An *atpE*-specific promoter within the coding region of the *atpB* gene in tobacco chloroplast DNA. Curr. Genet. **26**, 263–268.

Klein, R.R., and Mullet, J.E. (1990). Light-induced transcription of chloroplast genes: *psbA* transcription is differentially enhanced in illuminated barley. J. Biol. Chem. **265**, 1895–1902.

Klimyuk, V.I., Carolli, B.J., Thomas, C.M., and Jones, J.D.G. (1993). Alkali treatment for rapid preparation of plant material for reliable PCR analysis. Plant J. **3**, 493–494.

Kohchi, T., Yoshida, T., Komano, T., and Ohyama, K. (1988). Divergent mRNA transcription in the chloroplast *psbB* operon. EMBO J. **7**, 885–891.

Konieczny, A., and Ausubel, F.M. (1993). A procedure for mapping Arabidopsis mutations using co-dominant ecotype-specific PCR-based markers. Plant J. **4**, 403–410.

Koornneef, M., and Stam, P. (1992). Genetic analysis. In Methods in Arabidopsis Research, C. Koncz, N.-H. Chua, and J. Schell, eds (Singapore: World Scientific), pp. 83–99.

Krause, G.H., and Weis, E. (1991). Chlorophyll fluorescence and photosynthesis: The basics. Annu. Rev. Plant Physiol. Plant Mol. Biol. **42**, 313–349.

Krugh, B.K., and Miles, D. (1995). Energy transfer for low temperature fluorescence in PSII mutant thylakoids. Photosynth. Res. **44**, 117–125.

Kubicki, A., Steinmüller, K., and Westhoff, P. (1994). Differential transcription of plastome-encoded genes in the mesophyll and bundle-sheath chloroplasts of the monocotyledonous NADP-malic enzyme type C_4 plants maize and sorghum. Plant Mol. Biol. **25**, 669–679.

Kubicki, A., Funk, E., Westhoff, P., and Steinmüller, K. (1996). Differential expression of plastome-encoded *ndh* genes in mesophyll and bundle sheath chloroplasts of the C_4 plant *Sorghum bicolor* indicates that the complex I-homologous NAD(P)H-plastoquinone-oxidoreductase is involved in cyclic electron transport. Planta **199**, 276–281.

Kuchka, M.R., Goldschmidt-Clermont, M., van Dillewijn, J., and Rochaix, J.-D. (1989). Mutation at the Chlamydomonas nuclear *NAC2* locus specifically affects stability of the chloroplast *psbD* transcript encoding polypeptide D2 of PS II. Cell **58**, 869–876.

Lander, E.S., Green, P., Abrahamson, J., Barlow, A., Daly, M.J., Lincoln, S.E., and Newburg, L. (1987). MAPMAKER: An interactive computer package for constructing primary genetic linkage maps of experimental and natural populations. Genomics **1**, 174–181.

Li, Y., and Sugiura, M. (1991). Nucleic acid–binding specificities of tobacco chloroplast ribonucleoproteins. Nucleic Acids Res. **19**, 2893–2896.

Mans, R.J., and Novelli, G.D. (1961). Measurement of the incorporation of radioactive amino acids into protein by a filter-paper disk method. Arch. Biochem. Biophys. **94**, 48–53.

Matsubayashi, T., Wakasugi, T., Shinozaki, K., Yamaguchi-Shinozaki, K., Zaita, N., Hidaka, T., Meng, B.Y., Ohto, C., Tanaka, M., Kato, A., Maruyama, T., and Sugiura, M. (1987). Six chloroplast genes (*ndhA–F*) homologous to human mitochondrial genes encoding components of the respiratory chain NADH dehydrogenase are actively expressed: Determination of the splice sites *ndhA* and *ndhB* pre-mRNAs. Mol. Gen. Genet. **210**, 385–393.

Mayfield, S.P., Yohn, C.B., Cohen, A., and Danon, A. (1995). Regulation of chloroplast gene expression. Annu. Rev. Plant Physiol. Plant Mol. Biol. **46**, 147–166.

McMaster, G.K., and Carmichael, G.G. (1977). Analysis of single- and double-stranded nucleic acids on polyacrylamide and agarose gels by using glyoxal and acridine orange. Proc. Natl. Acad. Sci. USA **74**, 4835–4838.

Meierhoff, K., and Westhoff, P. (1993). Differential biogenesis of photosystem II in mesophyll and bundle-sheath cells of monocotyledonous NADP-malic enzyme-type C_4 plants: The non-stoichiometric abundance of the subunits of photosystem II in the bundle-sheath chloroplasts and the translational activity of the plastome-encoded genes. Planta **191**, 23–33.

Meurer, J., Meierhoff, K., and Westhoff, P. (1996). Isolation of high-chlorophyll-fluorescence mutants of *Arabidopsis thaliana* and their characterisation by spectroscopy, immunoblotting and northern hybridisation. Planta **198**, 385–396.

Miles, D. (1980). Mutants of higher plants: Maize. Methods Enzymol. **69**, 3–23.

Miles, D. (1982). The use of mutations to probe photosynthesis in higher plants. In Methods in Chloroplast Molecular Biology, M. Edelman, R.B. Hallik, and N.-H. Chua, eds (New York: Elsevier), pp. 75–106.

Monod, C., Goldschmidt-Clermont, M., and Rochaix, J.-D. (1992). Accumulation of chloroplast *psbB* RNA requires a nuclear factor in *Chlamydomonas reinhardtii*. Mol. Gen. Genet. **231**, 449–459.

Monod, C., Takahashi, Y., Goldschmidt-Clermont, M., and Rochaix, J.-D. (1994). The chloroplast *ycf8* open reading frame encodes a photosystem II polypeptide which maintains photosynthetic activity under adverse growth conditions. EMBO J. **13**, 2747–2754.

Mullet, J.E., and Klein, R.R. (1987). Transcription and RNA stability are important determinants of higher plant chloroplast RNA levels. EMBO J. **6**, 1571–1579.

Newbury, S.F., Smith, N.H., and Higgins, C.F. (1987). Differential mRNA stability controls relative gene expression within a polycistronic operon. Cell **51**, 1131–1143.

Nickelsen, J., and Link, G. (1993). The 54 kDa RNA-binding protein from mustard chloroplasts mediates endonucleolytic transcript 3′ end formation in vitro. Plant J. **3**, 537–544.

Nickelsen, J., van Dillewijn, J., Rahire, M., and Rochaix, J.-D. (1994). Determinants for stability of the chloroplast *psbD* RNA are located within its short leader region in *Chlamydomonas reinhardtii*. EMBO J. **13**, 3182–3191.

Offermann, K. (1988). Studien zu Struktur und Expression polycistronischer Transkriptionseinheiten für plastomkodierte Thylakoidmembranproteine. PhD Dissertation (Düsseldorf, Germany: Universität Düsseldorf).

Ohyama, K. (1992). Organization and expression of genes of plastid chromosomes from non-angiospermous land plants and green algae. In Plant Gene Research—Cell Organelles, R.G. Herrmann, ed (Vienna: Springer-Verlag), pp. 137–163.

Palmer, J.D. (1992). Comparison of chloroplast and mitochondrial genome evolution in plants. In Plant Gene Research—Cell Organelles, R.G. Herrmann, ed (Vienna: Springer-Verlag), pp. 99–133.

Pestka, S. (1971). Inhibitors of ribosome functions. Annu. Rev. Microbiol. **25,** 487–562.

Poetsch, W., Hermans, J., and Westhoff, P. (1991). Multiple cDNAs of phosphoenolpyruvate carboxylase in the C_4 dicot *Flaveria trinervia*. FEBS Lett. **292,** 133–136.

Reinbothe, S., Reinbothe, C., Heintzen, C., Seidenbecher, C., and Parthier, B. (1993). A methyl jasmonate–induced shift in the length of the 5′ untranslated region impairs translation of the plastid *rbcL* transcript in barley. EMBO J. **12,** 1505–1512.

Rochaix, J.-D. (1992). Post-transcriptional steps in the expression of chloroplast genes. Annu. Rev. Cell Biol. **8,** 1–28.

Sakamoto, W., Kindle, K.L., and Stern, D.B. (1993). In vivo analysis of Chlamydomonas chloroplast *petD* gene expression using stable transformation of β-glucuronidase translational fusions. Proc. Natl. Acad. Sci. USA **90,** 497–501.

Salvador, M.L., Klein, U., and Bogorad, L. (1993). 5′ Sequences are important positive and negative determinants of the longevity of Chlamydomonas chloroplast gene transcripts. Proc. Natl. Acad. Sci. USA **90,** 1556–1560.

Sambrook, J., Fritsch, E.F., and Maniatis, T. (1989). Molecular Cloning: A Laboratory Manual. (Cold Spring Harbor, NY: Cold Spring Harbor Laboratory).

Schägger, H., and von Jagow, G. (1987). Tricine-sodium dodecyl sulfate–polyacrylamide gel electrophoresis for the separation of proteins in the range from 1 to 100 kDa. Anal. Biochem. **166,** 368–379.

Schuster, G., and Gruissem, W. (1991). Chloroplast mRNA 3′ end processing requires a nuclear-encoded RNA-binding protein. EMBO J. **10,** 1493–1502.

Shen, G., Eaton-Rye, J.J., and Vermaas, W.F.J. (1993). Mutation of histidine residues in CP47 leads to destabilization of the photosystem II complex and to impairment of light energy transfer. Biochemistry **32,** 5109–5115.

Shinozaki, K., Ohme, M., Tanaka, M., Wakasugi, T., Hayashida, N., Matsubayashi, T., Zaita, N., Chunwongse, J., Obokata, J., Yamaguchi-Shinozaki, K., Ohto, C., Torazawa, K., Meng, B., Sugita, M., Deno, H., Kamogashira, T., Yamada, K., Kusuda, J., Takaiwa, F., Kato, A., Tohdoh, N., Shimada, H., and Sugiura, M. (1986). The complete nucleotide sequence of the tobacco chloroplast genome: Its gene organisation and expression. EMBO J. **5,** 2043–2049.

Sieburth, L.E., Berry-Lowe, S., and Schmidt, G.W. (1991). Chloroplast RNA stability in Chlamydomonas: Rapid degradation of *psbB* and *psbC* transcripts in two nuclear mutants. Plant Cell **3,** 175–189.

Somersalo, S., and Krause, G.H. (1990). Reversible photoinhibition of unhardened and cold-acclimated spinach leaves at chilling temperatures. Planta **180,** 181–187.

Somerville, C.R., Somerville, S.C., and Ogren, W.L. (1981). Isolation of photosynthetically active protoplasts and chloroplasts from *Arabidopsis thaliana*. Plant Sci. Lett. **21,** 89–96.

Steinkötter, J., Bhattacharya, D., Semmelroth, I., Bibeau, C., and Melkonian, M. (1994). Prasinophytes form independent lineages within the Chlorophyta: Evidence from ribosomal RNA sequence comparisons. J. Phycol. **30,** 340–345.

Steinmüller, K., Ley, A.C., Steinmetz, A.A., Sayre, R.T., and Bogorad, L. (1989). Characterization of the *ndhC-psbG-ORF157/159* operon of maize plastid DNA and of the cyanobacterium *Synechocystis* sp. PCC6803. Mol. Gen. Genet. **216,** 60–69.

Stern, D.B., and Gruissem, W. (1987). Control of plastid gene expression: 3′ Inverted repeats act as mRNA processing and stabilizing elements, but do not terminate transcription. Cell **51,** 1145–1157.

Stern, D.B., Radwanski, E.R., and Kindle, K.L. (1991). A 3′ stem/loop structure of the Chlamydomonas chloroplast *atpB* gene regulates mRNA accumulation in vivo. Plant Cell **3,** 285–297.

Sugiura, M. (1992). The chloroplast genome. Plant Mol. Biol. **19,** 149–168.

Takahashi, Y., Goldschmidt-Clermont, M., Soen, S.-Y., Franzén, L.G., and Rochaix, J.-D. (1991). Directed chloroplast transformation in *Chlamydomonas reinhardtii*: Insertional inactivation of the *psaC* gene encoding the iron sulfur protein destabilizes photosystem I. EMBO J. **10,** 2033–2040.

von Gabain, A., Belasco, J.G., Schottel, J.L., Chang, A.C.Y., and Cohen, S.N. (1983). Decay of mRNA in *Escherichia coli*: Investigation of the fate of specific segments of transcripts. Proc. Natl. Acad. Sci. USA **80,** 653–657.

Weis, E. (1985). Chlorophyll fluorescence at 77K in intact leaves: Characterization of a technique to eliminate artifacts related to self-absorption. Photosynth. Res. **6,** 73–86.

Westhoff, P. (1985). Transcription of the gene encoding the 51 kD chlorophyll *a*-apoprotein of the photosystem II reaction centre from spinach. Mol. Gen. Genet. **201,** 115–123.

Westhoff, P., and Herrmann, R.G. (1988). Complex RNA maturation in chloroplasts: The *psbB* operon from spinach. Eur. J. Biochem. **171,** 551–564.

Westhoff, P., Jansson, C., Klein-Hitpass, L., Berzborn, R., Larsson, C., and Bartlett, S.G. (1985). Intracellular coding sites of polypeptides associated with photosynthetic oxygen evolution of photosystem II. Plant Mol. Biol. **4,** 137–146.

Westhoff, P., Schrubar, H., Oswald, A., Streubel, M., and Offermann, K. (1990). Biogenesis of photosystem II in C_3 and C_4 plants—a model system to study developmentally regulated and cell-specific expression of plastid genes. In Current Research in Photosynthesis, Vol. 3, M. Baltscheffsky, ed (Dordrecht, The Netherlands: Kluwer Academic Publishers), pp. 483–490.

Westhoff, P., Offermann-Steinhard, K., Höfer, M., Eskins, K., Oswald, A., and Streubel, M. (1991). Differential accumulation of plastid transcripts encoding photosystem II components in the mesophyll and bundle-sheath cells of monocotyledonous NADP–malic enzyme–type C_4 plants. Planta **184,** 377–388.

Woodbury, N.W., Dobres, M., and Thompson, W.F. (1989). The identification and localization of 33 pea chloroplast transcription initiation sites. Curr. Genet. **16,** 433–445.

Yao, W.B., Meng, B.Y., Tanaka, M., and Sugiura, M. (1989). An additional promoter within the protein-coding region of the *psbD-psbC* gene cluster in tobacco chloroplast DNA. Nucleic Acids Res. **17,** 9583–9591.